Journal of Human Genetics (2019) 64:599–607
https://doi.org/10.1038/s10038-019-0601-9

ARTICLE

Identification of a novel *ANO5* missense mutation in a Chinese family with familial florid osseous dysplasia

Mingming Lv[1,2] · Guoling You[3] · Jinbing Wang[1,2] · Qihua Fu[3] · Anand Gupta[4] · Jun Li[1,2] · Jian Sun[1,2]

Received: 25 August 2018 / Revised: 23 March 2019 / Accepted: 5 April 2019 / Published online: 17 April 2019

Abstract

Familial florid osseous dysplasia (FFOD) is an autosomal dominant disorder of connective tissue, characterized by lobulated cementum-like masses scattered throughout the jaws and the alveolar process. This study aimed to identify the genetic etiology of a three-generation Chinese family affected with FFOD. A novel missense mutation p.C356W in anoctamin 5 (ANO5) gene was successfully identified as the pathogenic mutation by whole-exome sequencing (WES). The p.C356W mutation is located in the first loop between the first and second transmembrane domain of *ANO5* protein. Sequence alignment of *ANO5* protein among many different species revealed that this position is highly conserved. The p.C356W mutation may damage the predicted protein stability of *ANO5* by altering the structure of several extracellular loops of *ANO5* and affecting the formation of the disulfide bond, thereby disrupting the correct folding of *ANO5* protein. Thus, the amino acid at position 356 appears to play a key role in the protein structural stability and function of *ANO5* protein. Our results may also provide new insights into the cause and diagnosis of FFOD and may have implications for genetic counseling and clinical management.

Introduction

Familial florid osseous dysplasia, is a rare hereditary autosomal dominant skeletal disorder. It is a sclerosing disease, which is characterized by lobulated cementum-like masses scattered throughout the jaws and the alveolar process. In 1976, Melrose et al. first described florid osseous dysplasia (FOD) as a subtype of cemento-osseous dysplasia [1]. In 1985, Waldron proposed the use of the term "Florid Cemento-Osseous Dysplasia (FCOD)" because the sclerotic masses resemble the cementum [2]. In 2005, WHO classification recommends the use of the term "florid osseous dysplasia" (FOD) for this condition [3].

Familial form of FOD is rare, it was reported in a limited number of literature [4–7]. Nevertheless, no pathogenic mutations were reported. This study describes three generations of a family, diagnosed with FFOD. Whole-exome sequencing (WES) data analysis was performed in the affected members of this family and validated a novel mutation in the *ANO5* gene in all affected individuals.

Materials and methods

Ethics statement

The Ethics Institutional Committee of Ninth People's Hospital, Shanghai Jiao Tong University School of Medicine, reviewed and approved this study. Informed consent was obtained from all affected and control family members.

These authors contributed equally: Mingming Lv, Guoling You

✉ Jun Li
jinciyvlang@163.com

✉ Jian Sun
sunjian1960@126.com

[1] Department of Oral Maxillofacial-Head Neck Oncology, Shanghai Ninth People's Hospital, College of Stomatology, Shanghai Jiao Tong University School of Medicine, Shanghai, China

[2] National Clinical Research Center for Oral Diseases, Shanghai Key Laboratory of Stomatology & Shanghai Research Institute of Stomatology, Shanghai, China

[3] Department of Laboratory Medicine, Shanghai Children's Medical Center, Shanghai Jiao Tong University School of Medicine, Shanghai, China

[4] Department of Dentistry, Government Medical College Hospital, Chandigarh, India

DNA extraction, whole-exome capture, and sequencing

Genomic DNA (gDNA) was isolated from peripheral blood samples with the QIAamp DNA Blood Mini Kit (Qiagen, Germany). The concentration and purity of the gDNA were determined by the spectrophotometer (NanoDrop, USA).

Exome sequence capture was performed using the SureSelect Human All Exon V5 Kit (Agilent Technologies, USA) in accordance with the manufacturer's instructions. The capture library was sequenced via 2×150 paired-end sequencing on a Hiseq2000 Sequencer (Illumina, USA).

Analysis of sequencing data

Sequence reads were aligned to the human reference genome (hg19) using Burrows–Wheeler Aligner algorithm and then processed using SAMtools [8] and Picard toolkit (http://broadinstitute.github.io/picard). Single-nucleotide variations (SNVs) and small insertions/deletions (indels) were further analyzed using the Genome Analysis Toolkit (GATK) [9] and VarScan software [10]. Variants were annotated using the ANNOVAR program [11].

Variants with a low-quality score (depth <10 or genotype quality <20) were filtered. All variants present in a homozygous state were excluded; nonsense mutations and low-frequency frameshift mutations were considered pathogenic. Missense variants were analyzed using SIFT [12], Polyphen-2 [13], MutationTaster [14], FATHMM [15], PROVEAN [16], MetaSVM [17], MetaLR [17], REVEL [18], and M-CAP [19] for the assessment of any potentially damaging effects. The variants co-segregating with a model of an autosomal dominant disorder and genes annotated to be associated with skeletal disorders were prioritized and filtered. Variants that passed these filtering steps were considered as disease-causing mutations and were subsequently validated by Sanger sequencing.

Variant validation by Sanger sequencing

Following the results of exome sequencing, Sanger sequencing was performed to validate candidate FOD-causing variants in all available family members. The primers were designed by Primer3 [20] (PCR primers, PCR reaction conditions are available upon request). The PCR products were sequenced by ABI 3730XL DNA Sequencer (Applied Biosystems, USA), and the sequences were assembled and analyzed by Mutation Surveyor software (SoftGenetics, USA). We also tested the gDNA of 200 healthy controls.

Conservative analysis and molecular modeling of the *ANO5* protein

To estimate the evolutionary conservation of the mutated site, protein sequences of *ANO5* from ten animal species of fishes to mammals, including zebrafish (Danio rerio: XP_009 296468.1), gekko (Gekko japonicus: XP_015266713.1), frog (Xenopus laevis: XP_002933920.2), chicken (Gallus gallus: NP_001161856.1), mouse (Mus musculus: NP_808362.2), rat (Rattus norvegicus: XP_006229328.1), dog (Canis lupus: NP_001161885.1), cattle (Bos taurus: NP_001161878.1), pig (Sus scrofa: XP_005661129.2), and human (Homo sapiens: NP_998764.1) were aligned using ClustalW embedded in MEGA 7 [21].

The initial mutant protein structures for *ANO5* were constructed using the protein-homology modeling server MODELLER [22], using a cryo-EM structure of the mTMEM16A (PDB: 5NL2), an X-ray structure of a calcium-activated TMEM16 lipid scramblase (PDB: 4WIT and 4WIS) as a structural template. The analysis of the three-dimensional (3D) structure of the ANO5 proteins was carried out using PyMOL (https://pymol.org/2/). The cysteine oxidation state and disulfide bond connectivity of *ANO5* was determined by DiAminoacid Neural Network Application (DiANNA) [23].

Results

Clinical features

We recruited a family with an autosomal dominant FFOD in this study (Fig. 1). The family comprises three generations. The proband (II-3), a man of 49 years old, presented with several divided bulges involving all four quadrants of jaw (Fig. 2). His panoramic radiograph showed lobulated radiopaque areas around mandibular teeth roots with a "cloud-like" appearance. Nonetheless, the erupted teeth

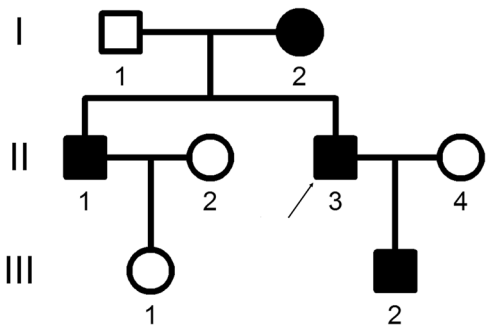

Fig. 1 Pedigree information of familial florid osseous dysplasia family. Generations are shown as I–III. Males are indicated by a square, females by circles, affected members indicated by a shaded black square or circles, and the proband (II-1) indicated by an arrow

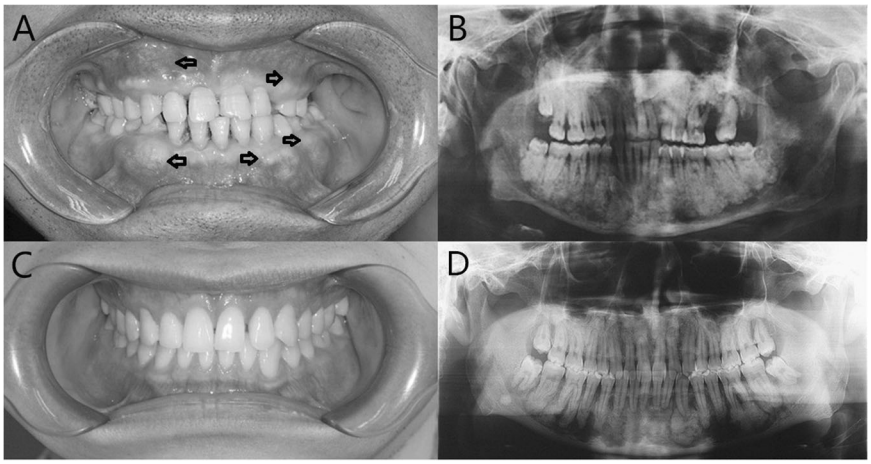

Fig. 2 Clinical appearance of an alveolar arch in the proband (II-3) showing multiple bony expansion (arrow, **a**); panoramic radiograph of the proband (II-3) showing the large, irregularly shaped, sclerotic radiopacities in the jaws (**b**); clinical appearance of an alveolar arch in the son of the proband (III-2) showing no bony expansion (**c**), while a panoramic radiograph showing irregularly shaped, sclerotic radiopacities in the jaws (**d**)

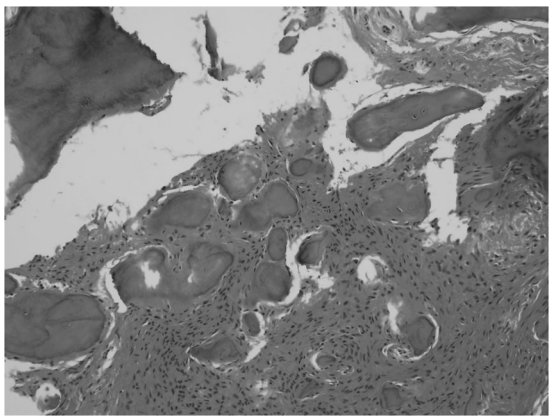

Fig. 3 The pathological image of FFOD for the proband (II-3). (HE, magnification ×400)

were normal. He was treated for inflammatory and osteonecrotic processes that occurred after teeth extractions which involved a molar area in the left maxilla, and the result of pathology was FFOD (Fig. 3). His mother (I-2), his brother, and his son (III-1) (Fig. 2) also showed such radiographic features through a panoramic radiograph. A segmental mandibulectomy was performed to his mother for osteomyelitis associated with fistula formation involving the mandible. His brother and son were totally asymptomatic and the lesions were detected on panoramic radiographs. The involvement of the lesions was limited to the jaws. No more pathological features were found in other anatomical sites on the proband or other affected family members (Fig. 4). Dual-energy X-ray absorptiometry (DXA), peripheral quantitative computed tomography, and laboratory tests for bone markers were assessed in the proband, his brother, and his son (Fig. 5). All the results of the skeletal status were normal. These results confirmed that the long bones are not affected by this lesion and the family is not affected by a mild manifestation of *ANO5*-associated gnathodiaphyseal dysplasia.

Identifying causal mutation for the FFOD pedigree

WES was performed for the identification of potential causative variant. A total of 79464694 and 76394186 reads were acquired from the two samples. The average coverage depth were 96.2× and 92.4×, which is sufficient depth to interrogate the exons for mutations. Of these, an average of 99.9% of the reads had Phred-like quality scores (Q scores) of >20 and 98.1% of the reads had Q scores of greater than 30. Variant calling generated 42830 and 40740 single-nucleotide variations (SNVs) in the exome prior to filtering, with 7146 and 6732 SNVs occurring in coding regions, respectively.

Variants were excluded if minor allele frequency (MAF) was more than 0.01 in the data from the 1000 Genomes Project, since the FFOD causative variants should be rare in the general population. Given the apparent autosomal dominant inheritance in this family, all homozygous variants were excluded from the analysis of FFOD-causing mutations. In addition, we removed all synonymous and intronic variants. As we expected, the causative variants would be shared by all affected individuals, and all variants not fulfilling this criterion were excluded. Prediction of deleterious non-synonymous SNVs for human diseases was performed by using different in silico tools, including SIFT, PolyPhen-2, MutationTaster, FATHMM, PROVEAN, MetaSVM, MetaLR, M-CAP, and REVEL. Finally, a solitary heterozygous missense variant, c.1068T>G (NM_213599) in exon 11 of the *ANO5* gene (Fig. 6), was identified in the proband (II-3) based on the OMIM database. This mutation is predicted to convert amino acid 356 from cysteine to tryptophan (p.C356W). This missense mutation was absent from the Human Gene Mutation Database (HGMD), dbSNP, TGP database and ESP6500 database, ClinVar database, Exome Aggregation Consortium (ExAC) database, and the Genome Aggregation Database (gnomAD).

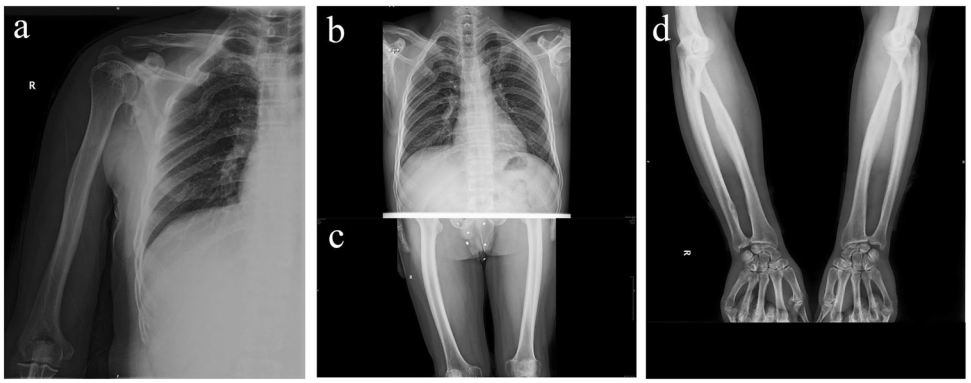

Fig. 4 X-rays showed that there was no other lesion or osteoporosis was found in limb bones and other anatomical sites of the proband or other affected family members. (**a** humerus; **b** chest; **c** femur; **d** ulna and radius)

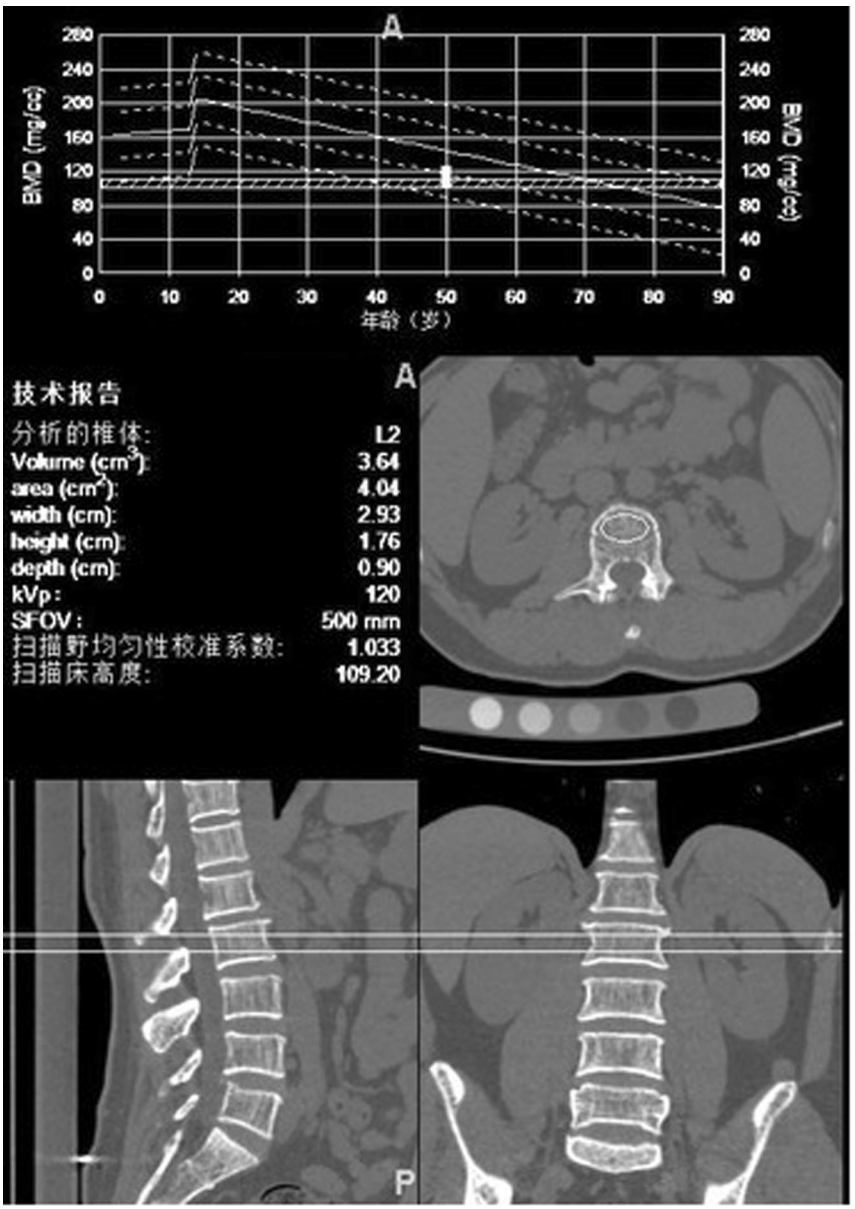

Fig. 5 Peripheral quantitative computed tomography showed bone mineral density (BMD) between 80 and 120 mg/cm^3 for the proband

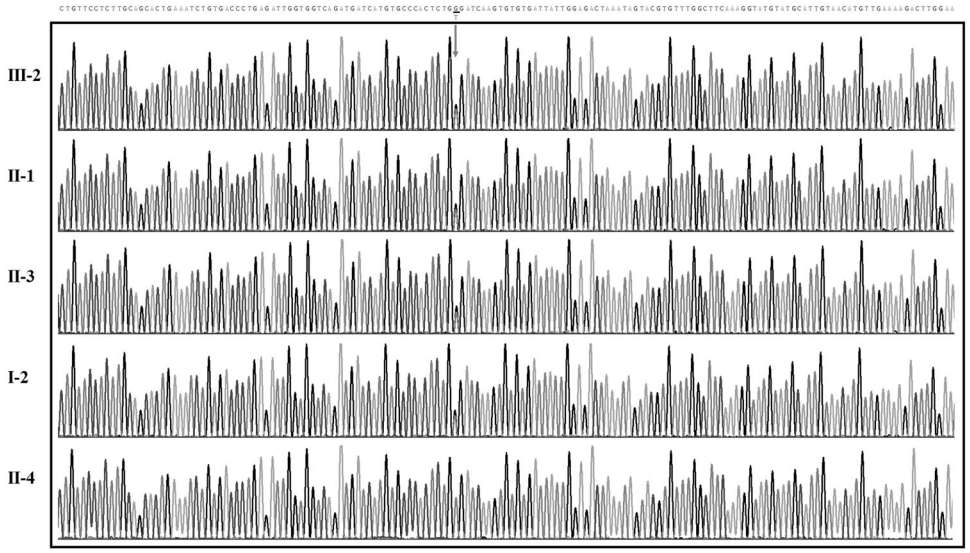

Fig. 6 Sanger sequencing to confirm the *ANO5*c.1068T>G mutation in the FFOD family members. The mutation is marked by a red arrow

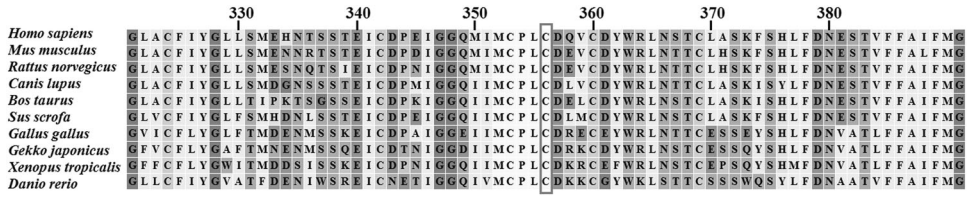

Fig. 7 Sequence conservation analysis of *ANO5* protein. Phylogenetic comparison of *ANO5* protein across species. Position of the mutation within a highly conserved region indicated with a red box

Variant validation by Sanger sequencing

The p.C356W mutation was also detected in other affected individuals (I-2, II-1, and III-2) by Sanger sequencing. The missense mutation was not identified in unaffected individuals (I-1, II-4, and III-1) (Figs. 1 and 6). The p.C356W mutation in the *ANO5* gene showed complete co-segregation with the clinical phenotype. In addition, it was further confirmed that this mutation was absent in the *ANO5* gene in 200 unrelated, ethnically and geographically matched controls, excluding the possibility of SNP.

Bioinformatics analysis

To further understand the role of mutant *ANO5* on protein structure and function, this mutation was analyzed in silico with SIFT, PolyPhen-2, MutationTaster, FATHMM, PROVEAN, MetaSVM, MetaLR, M-CAP, and REVEL to predict deleterious SNVs for human diseases. Based on this analysis, the p.C356W substitution was predicted to be deleterious, based on SIFT score (<0.05), FATHMM score (−1.52), PROVEAN score (–10.18), MetaSVMscore (0.307), and MetaLRscore (0.663), rated as "probably damaging" by PolyPhen2 with a score of 1.0, predicted as "disease causing" by MutationTaster analysis with a score of 1.0, classified as "pathogenic" by REVEL analysis with a score of 0.781 (close to 1.0), and by M-CAP analysis with a score of 0.581 (>0.025). Protein conservation analysis by an alignment of *ANO5* protein sequences revealed that this position is highly conserved among diverse species (Fig. 7). Thus, this amino acid appears to play a major role in the structure and function of *ANO5*.

We analyzed the predicted effects on the secondary structure of p.C356W mutation and other previously reported GDD mutations p.C356G, p.C356R, and p.C316Y on this site by MODELER. The transmembrane helix prediction is based on a recently published cryo-EM structure of the mTMEM16A (PDB: 5NL2) and X-ray structure of a calcium-activated TMEM16 lipid scramblase (PDB: 4WIT and 4WIS). The p.C356W mutation could affect the structural integrity and stability of the mutant *ANO5* protein (Fig. 8). By using PyMOL, we revealed that p.Cys356Trp mutation might affect the predicted structure of the protein by altering the structure of several extracellular loops of *ANO5* (Fig. 9). Residues Lys847, Phe848, and Leu849 are estimated to form a helix in wild type, p.Cys356Gly, p.Cys356Arg, and p.Cys316Tyr of *ANO5* protein, which are predicted to create a loop in the mutant p.Cys356Trp of *ANO5* protein. *ANO5* has 13 cysteines that form six disulfide bridges to support protein stability with connectivity patterns 1–3, 2–5, 4–12, 6–13, 7–11, and 8–9 (between cysteines 224 and 342, 324 and 356, 353 and 606, 360 and 804, 369 and 601, and 434 and 520) predicted by DiANNA. Cys324 and Cys356 form a disulfide bond, and the p.

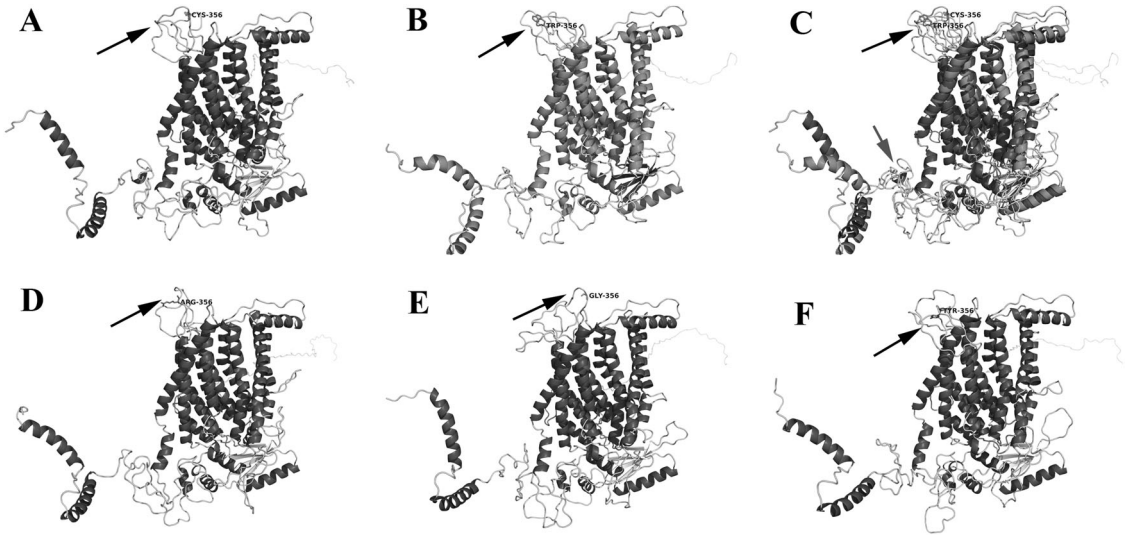

Fig. 8 Homology modeling of wild-type and mutant *ANO5* protein. **a** The wild-type ANO5 protein structure; **b** the p.Trp356 mutant *ANO5* protein structure; **c** 3D alignment of predicted structures of the wild-type *ANO5* protein and p.Trp356 mutant *ANO5* protein; **d** the p. Arg356 mutant *ANO5* protein structure; **e**: the p.Gly356 mutant *ANO5* protein structure; **f** the p.Tyr356 mutant *ANO5* protein structure

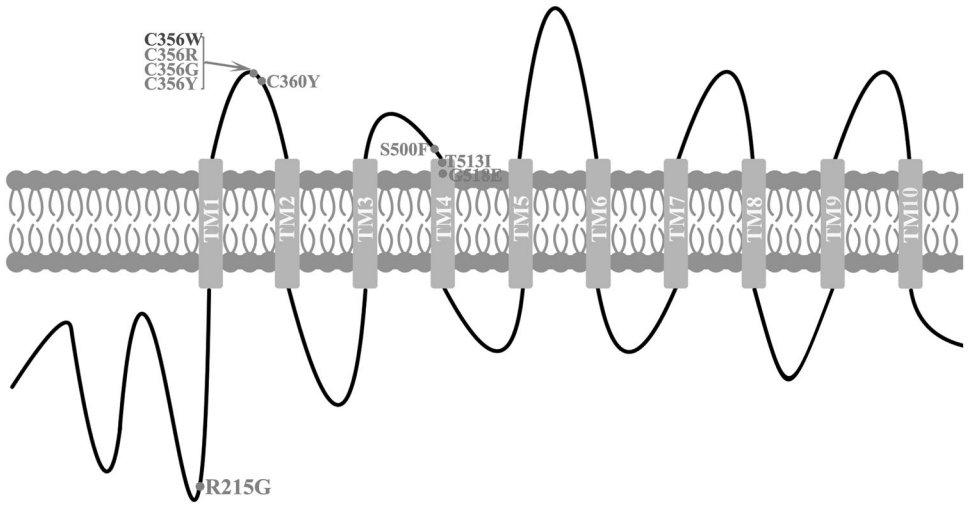

Fig. 9 Domain structure of *ANO5* protein. The *ANO5* protein consisted of ten transmembrane domains (TM), five extracellular loops, four intracellular loops, the amino terminus, and carboxyl terminus. The *ANO5* mutation is indicated as a red dot in the first extracelluar loop

C356W mutation is likely to damage disulfide bond formation, thereby disrupting the correct protein folding of *ANO5*.

Discussion

In this study, we report a novel heterozygous mutation p. C356W in the *ANO5* gene presented in a Chinese family with characteristic features of FFOD. It often involves both jaws bilaterally and develops slowly. Some papers say that the lesion preferentially affects the mandibular posterior region and occurs above the inferior alveolar nerve canal [5, 24, 25]. In our cases, panoramic radiographs showed a well-marginated radiopacity attached to the apices, occurred above the inferior alveolar nerve canal surrounding four quadrants along with bucco-lingual expansion of cortical plates.

FFOD generally progresses asymptomatically in the absence of infection. In some cases, the bone expansion can cause asymmetry of the face. Some serious cases suffer osteomyelitis, pain, and even bone sequestration due to odontogenic infections or sclerotic masses exposed to the oral cavity [26]. Similarly, in our cases, the proband and his mother came to our hospital with the complaint of suppuration due to osteomyelitis of the jaws.

According to the WHO classification (2005) (also updated WHO 2017) of osseous dysplasias (OD), FFOD is regarded as an odontogenic lesion that has the same periodontal ligament origin, as seen in familial gigantiform

cementoma (FGC), which is generally characterized by rapid and locally aggressive osseous expansion with predilection for young patients, causing severe malocclusion and facial disfigurement. Mainville et al. reported that in late stages of the disease, the sclerotic cemento-osseous masses of FGC have a high risk of becoming secondarily infected, which can lead to osteomyelitis, osteopenia, and bone fractures [27]. Unlike the previous reports of FGC, bony involvement by FFOD in our cases is limited to maxillofacial skeleton without obvious facial deformity, no osteopenia, and bone fractures. This characteristic was in accordance with the earlier reports of FFOD [28].

FFOD also shares similar clinical and pathological features with fibrous dysplasia. However, specific clinical features, histopathological entities, and genetic characteristics suggest that fibrous dysplasia is a distinct pathologic entity. Fibrous dysplasia and McCune–Albright syndrome are caused by activating pathogenic variants in *GNAS* (encoding the cAMP pathway-associated G protein, $G_s\alpha$). The genetic testing provides an important new approach to the diagnosis of FFOD and a potential tool to differentiate between these histopathologically similar but clinically distinct syndromes [29].

Mutations in the *ANO5* gene have been previously associated with gnathodiaphyseal dysplasia (GDD; OMIM: 166260). GDD is a rare autosomal dominant syndrome characterized by cemento-osseus lesions of the jawbones, in conjunction with frequent bone fractures and bowing of tubular bones at a young age. The fibro-osseous lesions in the jaws of GDD resemble cementum, which is similar with FOD. However, the clinical features in the tubular bones were different. Longbones in GDD usually appear osteosclerotic with thickened diaphysis and slightly undermodeled. By contrast, FFOD cases are limited to maxillofacial skeleton and no long bone fractures have been reported.

To date, only eight missense *ANO5* mutations have been reported to be associated with GDD [30–36]. Four mutations (p.Cys356Arg, p.Cys356Gly, p.Cys356Tyr, and p.Cys360Tyr) are known to be located in the first loop, between the first and second transmembrane domain of *ANO5* protein. Out of these, three mutations were identified in exon 11 at the same amino acid position (p.Cys356Arg, p.Cys356Gly, and p.Cys356Tyr). The p.Cys356Trp mutation identified in this research was first reported as the fourth genotype on this evolutionary-conserved site so far. This region neighbors the cavity formed by two *ANO5* dimerization subunits [34], but the functional significance of this region is currently unclear. The three-dimensional structure prediction indicates that p.Cys356Trp mutation may damage the predicted structure of the protein by altering the structure of the extracellular loops of *ANO5* and disturbing the disulfide bond formation, thereby disrupting the correct protein folding of *ANO5*. The mutation emphasizes the importance of this domain in *ANO5* function, at least in the pathogenesis of FFOD development. In contrast with GDD, the patients of FFOD have only a phenotype of florid osseous dysplasia of the jaws, and no other clinical and pathological features were detected in the affected individuals.

ANO5 encoding a 913-amino acid integral transmembrane protein and exhibiting ten transmembrane domains, is a member of the anoctamin protein family (Fig. 9). The family of anoctamin genes consists of 10 genes that share several regions of homology [33]. The anoctamin protein family is functionally split into Ca^{2+}-activated Cl^- channels and Ca^{2+}-activated phospholipid scramblases [37]. It is likely that *ANO5* may also have similar functions. ANO5 shows Ca^{2+}-dependent phospholipid scrambling activity and nonselective ion transport activity [37]. A recent report showed that GDD-causing T513I substitution is located in the second extracellular loop, and affects *ANO5* scrambling and ion transport activities [37]. However, it is unclear whether mutations in the first extracellular loop affect *ANO5* scrambling and ion transport activities. In addition, the biochemical properties and the molecular physiological function of *ANO5* mutations, leading to the skeletal and jaw manifestations, have not been fully elucidated. Further functional studies on the role of *ANO5* in bone pathophysiology are crucial for better understanding of the mechanism of this gene in GDD and FOD.

In addition to GDD and FOD, the human *ANO5* gene has also been reported to be associated with adult-onset muscle phenotypes, such as limb-girdle muscular dystrophy type 2 L (LGMD2L, OMIM 611307) and Miyoshi muscular dystrophy-like disease with a distal phenotype (MMD3, OMIM 613319) [38]. Till now, more than 70 different recessive *ANO5* gene mutations have been reported in muscular dystrophy patients, and are believed to cause a loss-of-function phenotype [39]. In humans, *ANO5* is highly expressed in only skeletal muscle and bone tissues, such as calvaria, femur, and mandible [40]. *ANO5* was identified as an unstable protein, which undergoes constitutive proteasomal degradation [41]. It seems that mutations in the *ANO5* gene further decrease the protein stability, either by misfolding, compromising its processing in the endoplasmic reticulum, or affecting its proper incorporation into membranes, resulting in more rapid degradation and decreased *ANO5* levels [42]. However, it cannot be ruled out that some mutations may primarily damage protein functionality. Different mutations leading to *ANO5* instability and degradation could not manifest as clear genotype–phenotype correlation. The different expression patterns of *ANO5* in the muscle cells and bone during the embryonic development and cellular differentiation might be one of the explanations

why the loss-of-function recessive mutations in *ANO5* lead to muscular dystrophy phenotype but do not affect the bone tissue [34]. Conversely, based on the model of inheritance and the absence of the overlap phenotype with muscular dystrophies, GDD-associated mutations may increase phenotype's function [37]. Mutations in the *ANO5* gene co-segregate with an autosomal dominant pathogenic phenotype related to the bone tissue, but not to the muscle tissue [34]. Along with previous reports, our data illuminate the significance of mutations in a single amino-acid position p.Cys356 of *ANO5* for a particular bone tissue pathology. For sure, a wider spectrum of different *ANO5* mutations needs to be analyzed to see how they affect protein function and what impact they have at the protein level.

In summary, we successfully identified a novel missense mutation p.C356W in the *ANO5* gene as the pathogenic mutation for FFOD by WES. The p.Cys356Trp mutation may affect the predicted structure of the protein by altering the structure of several extracellular loops of *ANO5* and affecting disulfide bond formation, thereby disrupting the correct protein folding of *ANO5*. Thus, this amino acid appears to play a crucial role in the structure and function of *ANO5*. These results offer a new perspective for the etiology and diagnostic methods of FFOD and may pave the way for genetic counseling and clinical management.

Acknowledgements This research was supported by The National Key Research and Development Program of China (2016YFC0902700), Shanghai Municipal Commission of Health and Family Planning (20174Y0025), Training Program for Clinical Medical Young Talents of Shanghai (to Guoling You), Chen Xing Excellent Young Teacher Training Program of Shanghai Jiao Tong University (to Guoling You), and the National Natural Science Foundation of China (81601847). We thank the patients and family members for their participation in this study.

Author contributions ML and GY performed the experiments; ML, GY, JL, and Jinbing Wang analyzed the data; GY, AG, and ML wrote and polished the paper; QF, JL, and JS conceived and supervised the experiments.

Compliance with ethical standards

Conflict of interest The authors declare that they have no conflict of interest.

Publisher's note: Springer Nature remains neutral with regard to jurisdictional claims in published maps and institutional affiliations.

References

1. Melrose RJ, Abrams AM, Mills BG. Florid osseous dysplasia. a clinical-pathologic study of thirty-four cases. Oral Surg Oral Med Oral Pathol. 1976;41:62–82.
2. Waldron CA. Fibro-osseous lesions of the jaws. J Oral Maxillofac Surg. 1985;43:249–62.
3. Thompson L. World Health Organization classification of tumours: pathology and genetics of head and neck tumours. Ear Nose Throat J. 2006;85:74.
4. Toffanin A, Benetti R, Manconi R. Familial florid cemento-osseous dysplasia: a case report. J Oral Maxillofac Surg. 2000;58:1440–6.
5. Mangala M, Ramesh DN, Surekha PS, Santosh P. Florid cemento-osseous dysplasia: review and report of two cases. Indian J Dent Res. 2006;17:131–4.
6. Kucukkurt S, Rzayev S, Baris E, Atac MS. Familial florid osseous dysplasia: a report with review of the literature. BMJ Case Rep. 2016. https://doi.org/10.1136/bcr-2015-214162
7. Thorawat A, Kalkur C, Naikmasur VG, Tarakji B. Familial florid Cemento-osseous dysplasia—case report and review of literature. Clin Case Rep. 2015;3:1034–7.
8. Li H, Durbin R. Fast and accurate long-read alignment with Burrows-Wheeler transform. Bioinformatics . 2010;26:589–95.
9. McKenna A, Hanna M, Banks E, Sivachenko A, Cibulskis K, Kernytsky A, et al. The Genome Analysis Toolkit: a MapReduce framework for analyzing next-generation DNA sequencing data. Genome Res. 2010;20:1297–303.
10. Koboldt DC, Zhang Q, Larson DE, Shen D, McLellan MD, Lin L, et al. VarScan 2: somatic mutation and copy number alteration discovery in cancer by exome sequencing. Genome Res. 2012;22:568–76.
11. Wang K, Li M, Hakonarson H. ANNOVAR. functional annotation of genetic variants from high-throughput sequencing data. Nucleic Acids Res. 2010;38:e164. https://doi.org/10.1093/nar/gkq603
12. Kumar P, Henikoff S, Ng PC. Predicting the effects of coding non-synonymous variants on protein function using the SIFT algorithm. Nat Protoc. 2009;4:1073–81.
13. Adzhubei I, Jordan DM, Sunyaev SR. Predicting functional effect of human missense mutations using PolyPhen-2. Curr Protoc Hum Genet. 2013;Chapter 7:Unit7 20.
14. Schwarz JM, Rodelsperger C, Schuelke M, Seelow D. MutationTaster evaluates disease-causing potential of sequence alterations. Nat Methods. 2010;7:575–6.
15. Shihab HA, Gough J, Cooper DN, Day IN, Gaunt TR. Predicting the functional consequences of cancer-associated amino acid substitutions. Bioinformatics. 2013;29:1504–10.
16. Choi Y, Chan AP. PROVEAN web server: a tool to predict the functional effect of amino acid substitutions and indels. Bioinformatics. 2015;31:2745–7.
17. Dong C, Wei P, Jian X, Gibbs R, Boerwinkle E, Wang K, et al. Comparison and integration of deleteriousness prediction methods for nonsynonymous SNVs in whole exome sequencing studies. Hum Mol Genet. 2015;24:2125–37.
18. Ioannidis NM, Rothstein JH, Pejaver V, Middha S, McDonnell SK, Baheti S, et al. REVEL: an ensemble method for predicting the pathogenicity of rare missense variants. Am J Hum Genet. 2016;99:877–85.
19. Jagadeesh KA, Wenger AM, Berger MJ, Guturu H, Stenson PD, Cooper DN, et al. M-CAP eliminates a majority of variants of uncertain significance in clinical exomes at high sensitivity. Nat Genet. 2016;48:1581–6.
20. Untergasser A, Cutcutache I, Koressaar T, Ye J, Faircloth BC, Remm M, et al. Primer3-new capabilities and interfaces. Nucleic Acids Res. 2012;40:e115.
21. Kumar S, Stecher G, Tamura K. MEGA7: molecular evolutionary genetics analysis version 7.0 for bigger datasets. Mol Biol Evol. 2016;33:1870–4.
22. Marti-Renom MA, Stuart AC, Fiser A, Sanchez R, Melo F, Sali A. Comparative protein structure modeling of genes and genomes. Annu Rev Biophys Biomol Struct. 2000;29:291–325.

23. Ferre F, Clote P. DiANNA 1.1: an extension of the DiANNA web server for ternary cysteine classification. Nucleic Acids Res. 2006;34(Web Server issue):W182–185.
24. Kawai T, Hiranuma H, Kishino M, Jikko A, Sakuda M. Cemento-osseous dysplasia of the jaws in 54 Japanese patients: a radiographic study. Oral Surg Oral Med Oral Pathol Oral Radio Endod. 1999;87:107–14.
25. Baden E, Saroff SA. Periapical cemental dysplasia and periodontal disease. A case report with review of the literature. J Periodontol. 1987;58:187–91.
26. Singer SR, Mupparapu M, Rinaggio J. Florid cemento-osseous dysplasia and chronic diffuse osteomyelitis Report of a simultaneous presentation and review of the literature. J Am Dent Assoc. 2005;136:927–31.
27. Mainville GN, Turgeon DP, Kauzman A. Diagnosis and management of benign fibro-osseous lesions of the jaws: a current review for the dental clinician. Oral Dis. 2017;23:440–50.
28. Bhaskar SN, Cutright DE. Multiple enostosis. report of 16 cases. J Oral Surg. 1968;26:321–6.
29. Riminucci M, Collins MT, Corsi A, Boyde A, Murphey MD, Wientroub S, et al. Gnathodiaphyseal dysplasia: a syndrome of fibro-osseous lesions of jawbones, bone fragility, and long bone bowing. J Bone Min Res. 2001;16:1710–8.
30. Marconi C, Brunamonti Binello P, Badiali G, Caci E, Cusano R, Garibaldi J, et al. A novel missense mutation in ANO5/TMEM16E is causative for gnathodiaphyseal dyplasia in a large Italian pedigree. Eur J Hum Genet: Ejhg. 2013;21:613–9.
31. Tsutsumi S, Kamata N, Vokes TJ, Maruoka Y, Nakakuki K, Enomoto S, et al. The novel gene encoding a putative transmembrane protein is mutated in gnathodiaphyseal dysplasia (GDD). Am J Hum Genet. 2004;74:1255–61.
32. Vengoechea J, Carpenter L. Gnathodiaphyseal dysplasia presenting as polyostotic fibrous dysplasia. Am J Med Genet Part A. 2015;167:1421–2.
33. Duong HA, Le KT, Soulema AL, Yueh RH, Scheuner MT, Holick MF, et al. Gnathodiaphyseal dysplasia: report of a family with a novel mutation of the ANO5 gene. Oral Surg Oral Med Oral Pathol Oral Radiol. 2016;121:e123–128.
34. Andreeva TV, Tyazhelova TV, Rykalina VN, Gusev FE, Goltsov AY, Zolotareva OI, et al. Whole exome sequencing links dental tumor to an autosomal-dominant mutation in ANO5 gene associated with gnathodiaphyseal dysplasia and muscle dystrophies. Sci Rep. 2016;6:26440. https://doi.org/10.1038/srep26440
35. Jin L, Liu Y, Sun F, Collins MT, Blackwell K, Woo AS, et al. Three novel ANO5 missense mutations in Caucasian and Chinese families and sporadic cases with gnathodiaphyseal dysplasia. Sci Rep. 2017;7:40935. https://doi.org/10.1038/srep40935
36. Rolvien T, Koehne T, Kornak U, Lehmann W, Amling M, Schinke T, et al. A novel ANO5 mutation causing gnathodiaphyseal dysplasia with high bone turnover osteosclerosis. J Bone Miner Res: Off J Am Soc Bone Miner Res. 2017;32:277–84.
37. Di Zanni E, Gradogna A, Scholz-Starke J, Boccaccio A. Gain of function of TMEM16E/ANO5 scrambling activity caused by a mutation associated with gnathodiaphyseal dysplasia. Cell Mol Life Sci. 2018;75:1657–70.
38. Liewluck T, Winder TL, Dimberg EL, Crum BA, Heppelmann CJ, Wang Y, et al. ANO5-muscular dystrophy: clinical, pathological and molecular findings. Eur J Neurol. 2013;20:1383–9.
39. Griffin DA, Johnson RW, Whitlock JM, Pozsgai ER, Heller KN, Grose WE, et al. Defective membrane fusion and repair in Anoctamin5-deficient muscular dystrophy. Hum Mol Genet. 2016;25:1900–11.
40. Mizuta K, Tsutsumi S, Inoue H, Sakamoto Y, Miyatake K, Miyawaki K, et al. Molecular characterization of GDD1/TMEM16E, the gene product responsible for autosomal dominant gnathodiaphyseal dysplasia. Biochem Biophys Res Commun. 2007;357:126–32.
41. Xu J, El Refaey M, Xu L, Zhao L, Gao Y, Floyd K, et al. Genetic disruption of Ano5 in mice does not recapitulate human ANO5-deficient muscular dystrophy. Skeletal muscle. 2015; 5:43. Skelet Muscle. 2015;5:43. https://doi.org/10.1186/s13395-015-0069-z
42. Vihola A, Luque H, Savarese M, Penttila S, Lindfors M, Leturcq F, et al. Diagnostic anoctamin-5 protein defect in patients with ANO5-mutated muscular dystrophy. Neuropathol Appl Neurobiol. 2017. https://doi.org/10.1111/nan.12410